



University of Guilan

journal homepage: <https://cse.guilan.ac.ir/>

## A computational multiscale investigation of buckling behavior for single-walled carbon nanotube/polymer nanocomposite beams

M.K. Hassanzadeh-Aghdam<sup>a,\*</sup>, M.J. Mahmoodi<sup>b</sup>

<sup>a</sup> Department of Engineering Science, Faculty of Technology and Engineering, East of Guilan, University of Guilan, Rudsar-Vajargah, Iran

<sup>b</sup> Faculty of Civil, Water and Environmental Engineering, Shahid Beheshti University, Iran

### ARTICLE INFO

#### Article history:

Available online 26 March 2021

#### Keywords:

Nanocomposite beam  
Buckling  
Computational analysis  
Finite element method

### ABSTRACT

In this paper, the buckling response of single-walled carbon nanotube (SWCNT) -reinforced shape memory polymer nanocomposite beams is investigated through a computational multiscale approach. First, the Mori-Tanaka micromechanical model is used to extract the effective mechanical properties of SWCNT-polymer nanocomposites. The role of interfacial region between the nanotubes and polymer matrix in the elastic properties is taken into account in the analysis. Then, the buckling behavior of the nanocomposite beams is evaluated by the finite element method (FEM). The effects of nanotube content, interphase and temperature on the buckling response are investigated. It is observed that the addition of SWCNT into the polymeric materials increases the buckling capacity of the resulting nanocomposite beams. According to the results, the buckling characteristics of shape memory polymer nanocomposite beams are affected by the CNT/polymer interphase. The increase of temperature significantly decreases the buckling loads of nanocomposite beams due to the decrease of nanocomposite elastic modulus.

## 1. Introduction

Carbon nanotubes (CNTs) are subject of extreme research, primarily due to their extraordinary strength, high stiffness, high aspect ratio, low density and multifunctional characteristics [1-3]. The CNTs as reinforcing agents are added into the polymeric materials to produce nanocomposites [4,5]. The emergence of CNT-reinforced polymer matrix nanocomposites with their unique mechanical and physical properties has led to numerous advances in a variety of engineering applications [6,7]. On the basis of tensile tests made by Qian et al. [8], it has been revealed that addition of 1 wt% CNT

\* Corresponding author.

E-mail addresses: [mk.hassanzadeh@gmail.com](mailto:mk.hassanzadeh@gmail.com) (M.K. Hassanzadeh-Aghdam)

into the polystyrene matrix results in 36%-42% and ~25% increases in Young's modulus and breaks stress, respectively. Jia et al. [9] have found that Young's modulus of polypropylene nanocomposites with content of 0.3 vol.% and 2.8 vol.% CNT can be increased by 15% and 32%, respectively, as compared to the pure polypropylene. The elastic modulus of poly(ether ether ketone) (PEEK) and 5 wt% CNT-reinforced PEEK nanocomposites has been measured to be  $1019.12 \pm 5.1$  MPa and  $1333.1 \pm 6.67$  MPa [10].

In the field of predicting effective properties of CNT-reinforced nanocomposites, micromechanical models such as the method of cell [11], simplified unit cell model [12], Halpin-Tsai [13] and Mori-Tanaka [14] are broadly utilized. For example, Pakseresht et al. [15] used the high-fidelity generalized method of cells to calculate the damping properties of aligned CNT-epoxy nanocomposites. Hassanzadeh-Aghdam et al. [16] extracted the thermo-elastic properties of CNT-reinforced shape memory polymer nanocomposites via the simplified unit cell micromechanical model. Haghgoo et al. [17] developed a micromechanical method based on the Mori-Tanaka model to comprehensively analyze the effect of thermal residual stresses on the overall elastoplastic behavior of the CNT-reinforced aluminum nanocomposites.

Composite beams are very important structural components. Such structures are extensively utilized in various industrial applications such as civil, architectural, aerospace and marine engineering and are often subjected to external loads that cause buckling. Consequently, investigation of buckling behavior of the CNT-reinforced composite structures is an essential research which will be helpful for optimum design [18-20]. Yas and Samadi [21] studied free vibration and buckling behaviors of single-walled carbon nanotube (SWCNT)-reinforced nanocomposite Timoshenko beams. Rafiee et al. [22] examined thermal bifurcation buckling characteristics of CNT-reinforced composite beams with surface-bonded piezoelectric layers. Based on several higher-order shear deformation theories, Wattanasakulpong and Ungbhakorn [23] evaluated bending, buckling and vibration responses of polymer matrix composite beams reinforced by different patterns of SWCNTs. Ahmadi et al. [5] investigated the buckling behavior of rods made of carbon fiber/CNT-reinforced polyimide composites subjected to action of axial load on the basis of a multi-scale finite element approach. The effects of volume fraction of reinforcements, interphase, and geometrical characteristics on the axial buckling response of the composite rods were studied.

Aim of present work is to analyze buckling response of SWCNT-reinforced shape memory polymer nanocomposite beam structures by a computational multiscale modeling approach. The effective material properties of nanocomposites in presence of CNT/polymer interphase region are estimated according to the Mori-Tanaka micromechanical model. Based on the finite element method (FEM), buckling characteristics of SWCNT/polymer nanocomposite beams are determined. The influences of CNT volume fraction, interphase and temperature on the buckling behavior of such beam structures are investigated.

## 2. Micromechanical modeling

On the basis of the Mori-Tanaka method [24-27], effective stiffness tensor of aligned CNT-reinforced nanocomposites can be given by

$$\mathbf{C}^{nc} = \{f_m[\mathbf{C}^m] + f_r[\mathbf{C}^r][\mathbf{A}]\}\{f_m[\mathbf{I}] + f_r[\mathbf{A}]\}^{-1} \quad (1)$$

in which  $f_r$  and  $f_m$  denote volume fractions of CNT and matrix, respectively,  $\mathbf{I}$  is the fourth-order identity tensor, and  $\mathbf{C}^m$  and  $\mathbf{C}^r$  signify stiffness tensors of matrix and CNT, respectively. Also,  $\mathbf{A}$  is defined as [24-27]

$$\mathbf{A} = [\mathbf{I} + \hat{\mathbf{S}}[\mathbf{C}^m]^{-1}([\mathbf{C}^r] - [\mathbf{C}^m])]^{-1} \quad (2)$$

in which the non-zero components of Eshelby tensor  $\hat{\mathbf{S}}$  are expressed as follows

$$\begin{aligned} s_{1111} = s_{3333} &= \frac{5 - 4\nu_m}{8(1 - \nu_m)}, & s_{1133} = s_{3311} &= \frac{4\nu_m - 1}{8(1 - \nu_m)} \\ s_{1122} = s_{3322} &= \frac{\nu_m}{2(1 - \nu_m)}, & s_{2323} = s_{1212} &= \frac{1}{4}, & s_{1313} &= \frac{3 - 4\nu_m}{8(1 - \nu_m)}. \end{aligned} \quad (3)$$

When CNTs are randomly oriented in the polymer matrix, the bulk modulus and shear modulus of the nanocomposite are derived as [24-27]

$$K^{nc} = K_m + \frac{f_r(\delta_r - 3K_m\alpha_r)}{3(f_m + f_r\alpha_r)} \quad (4)$$

$$G^{nc} = G_m + \frac{f_r(\eta_r - 2G_m\beta_r)}{2(f_m + f_r\beta_r)} \quad (5)$$

where

$$\alpha_r = \frac{3(K_m + G_m) + k_r - l_r}{3(G_m + k_r)} \quad (6)$$

$$\beta_r = \frac{1}{5} \left\{ \frac{4G_m + 2k_r + l_r}{3(G_m + k_r)} + \frac{4G_m}{G_m + p_r} + \frac{2[G_m(3K_m + G_m) + G_m(3K_m + 7G_m)]}{G_m(3K_m + G_m) + m_r(3K_m + 7G_m)} \right\} \quad (7)$$

$$\delta_r = \frac{1}{3} \left[ n_r + 2l_r + \frac{(2k_r + l_r)(3K_m + 2G_m - l_r)}{G_m + k_r} \right] \quad (8)$$

$$\eta_r = \frac{1}{5} \left[ \frac{2}{3}(n_r - l_r) + \frac{8G_m p_r}{G_m + p_r} + \frac{8m_r G_m (3K_m + 4G_m)}{3K_m(m_r + G_m) + G_m(7m_r + G_m)} + \frac{2(k_r - l_r)(2G_m + l_r)}{3(G_m + k_r)} \right] \quad (9)$$

in which  $K_m$  and  $G_m$  are the bulk modulus and shear modulus of the matrix, respectively. Also,  $k_r$ ,  $n_r$ ,  $l_r$ ,  $p_r$  and  $m_r$  are the Hill's elastic moduli of the reinforcing phase [24]. Young's modulus and Poisson's ratio of randomly oriented CNT-reinforced nanocomposite are given by

$$E^{nc} = \frac{9K^{nc}G^{nc}}{3K^{nc} + G^{nc}}, \quad \nu^{nc} = \frac{3K^{nc} - 2G^{nc}}{6K^{nc} + 2G^{nc}} \quad (10)$$

Density of the CNT/polymer nanocomposites is calculated as follows

$$\rho_{nc} = \rho_m f_m + \rho_r f_r \quad (11)$$

where  $\rho_m$  and  $\rho_r$  are densities of the matrix and CNT, respectively.

In a CNT-reinforced polymer matrix nanocomposite, non-bonding interaction between the CNT and surrounding matrix can affect its mechanical properties [15,16,25]. In the micromechanical modeling of nanocomposites, an interphase region is presented between the CNT and polymer matrix to characterize the degree of non-bonded interaction. The effective stiffness tensor of the interphase region is expressed as follows [16]

$$\mathbf{c}^i = \frac{1}{t_i} \int_{\frac{d}{2}}^{\frac{d}{2}+t_i} \mathbf{c}^m \left( \frac{d}{2} + t_i \right) + \left( \frac{d}{2} + t_i - r \right)^\eta \left[ \mathbf{c}^r - \mathbf{c}^r \left( \frac{d}{2} + t_i \right) \right] dr. \quad (12)$$

where  $t_i$  and  $d$  are interphase thickness and CNT diameter, respectively, and  $\eta$  is adhesion exponent. The CNT and interphase region can be virtually converted into an equivalent solid fiber as a single inclusion and its effective properties are obtained by the Mori-Tanaka model.

### 3. Finite element analysis

To investigate buckling behavior, finite element analysis is accomplished by means of commercial software ABAQUS package. The structure under consideration is a beam made of the SWCNT-reinforced polymer nanocomposite. The length of this nanocomposite beam is 1 m and its cross-section is  $0.1 \times 0.1$  m, as shown in Figure 1.

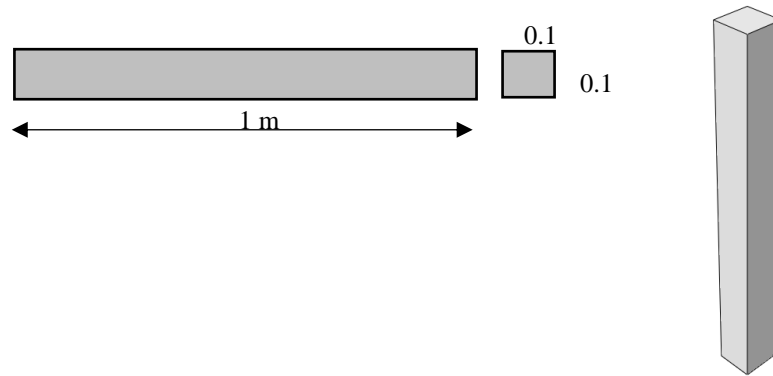


*Figure 1.* Dimensional characteristics of CNT/polymer nanocomposite beam

The boundary conditions imposed on the nanocomposite beam are shown in Figure 2.



*Figure 2.* Boundary conditions of the nanocomposite beam

The lower end of nanocomposite beam is assumed to be under clamped boundary condition. The upper end of nanocomposite beam is subjected to an axial pressure. The C3D20: A 20-node quadratic brick element is used to mesh the beam at the macro-scale. The meshed configuration is indicated in Figure 3. The size of element is 0.01 m.



Figure 3. Meshed configuration of nanocomposite beam

#### 4. Results and discussion

The nanocomposite system considered in this analysis consists of SWCNTs embedded in the shape memory polymer matrix. The mechanical properties of CNT are tabulated in Table 1 [28].

Table 1. Mechanical properties of CNT [28]

$E_L$ (GPa)	$G_L$ (GPa)	$\nu_L$	$E_T$ (GPa)	$G_T$ (GPa)
1060	442	0.162	50	17

The elastic modulus of shape memory polymer is given as [29]

$$E = \frac{1}{\frac{\varphi_f}{E_i} + \frac{1 - \varphi_f}{kT}}, \varphi_f = 1 - \frac{1}{1 + c_f(T_h - T)^n} \quad (13)$$

where  $T$  denotes the temperature. Other material properties of the shape memory polymer are mentioned in Table 2 [29].

Table 2. Material properties of shape memory polymer [29]

$c_f$ (K <sup>-4</sup> )	$T_h$ (K)	$E_i$ (MPa)	$k$ (MPa/K)	$n$	$\nu$
$2.76 \times 10^{-5}$	358	813	$2.64 \times 10^{-2}$	4	0.3

Figure 4 shows variation of elastic moduli of aligned SWCNT-reinforced shape memory polymer nanocomposites with nanotube volume fraction. The results are extracted in the presence and absence of interphase region. It is found that elastic moduli of polymer nanocomposites increase with increase of CNT volume fraction. Also, elastic modulus of nanocomposites in the presence of interphase is higher than that of the nanocomposite in absence of interphase.

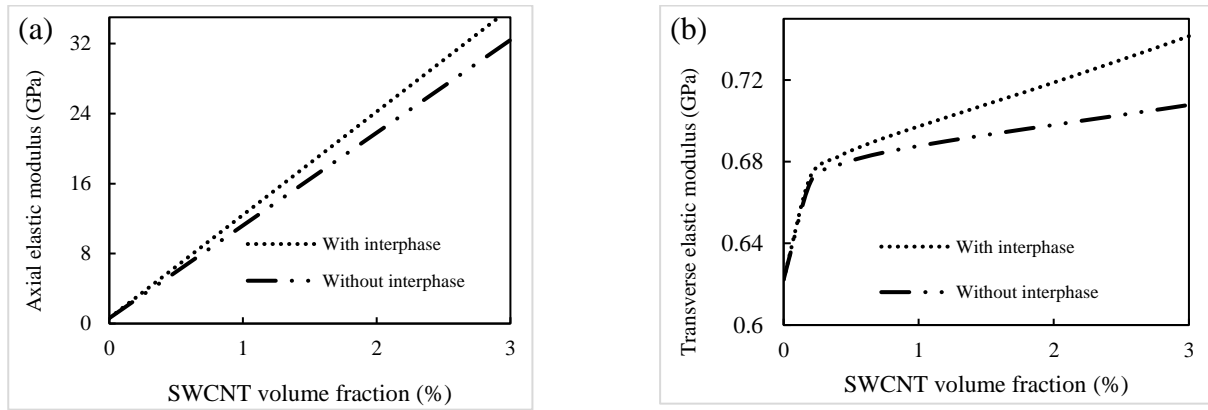


**Figure 4.** (a) Axial and (b) transverse elastic moduli of shape memory polymer nanocomposites versus the SWCNT volume fraction

Table 3 shows the buckling loads of SWCNT/polymer nanocomposite beams. Effects of interphase and nanotube volume fraction on the buckling behavior of nanocomposite beams are investigated. It is seen that with increase of SWCNT volume fraction, resistance of beams to applied axial load improves, significantly. Furthermore, presence of CNT/polymer interphase region leads to an increase in the buckling loads.

**Table 3.** Buckling load (MPa) of nanocomposite beams at different CNT contents

Volume fraction (%)	0	1	2	3	4	5
Without interphase	2.65	10.3	17.86	25.43	32.99	40.55
With interphase	2.65	11.21	19.69	28.17	36.64	45.12

Table 4 depicts effect of temperature on the buckling behavior of SWCNT/polymer nanocomposite beams. The results are extracted in presence and absence of interphase. It is observed that the buckling load of nanocomposite beams decreases as the temperature increases. It is due to decrease of nanocomposite elastic modulus by increase of temperature.

**Table 4.** Buckling load (MPa) of nanocomposite beams at different temperatures

Temperature (K)	260	280	300	320	340
Without interphase	41.28	41.06	40.46	38.99	37.73
With interphase	45.91	45.67	45.01	43.41	42.01

A mesh sensitivity analysis is performed to study the role of number of elements in the buckling behavior of SWCNT/polymer nanocomposite beams. The results are shown in Table 5.

**Table 5.** Effect of number of elements on the buckling load (MPa) of nanocomposite beams

Number of elements	5312	46541	95060
	28.43	28.17	27.87

## 5. Conclusions

The buckling behavior of SWCNT-reinforced polymer nanocomposite beams was studied by means of a computational multiscale approach. Effective material properties of nanocomposites were obtained by the Mori-Tanaka micromechanical model. The interfacial interaction between the CNT and polymer matrix was considered in the micromechanical analysis. The FEM was used to evaluate the buckling response of the nanocomposite beams. The results revealed that there was a notable improvement in the buckling capacity of the nanocomposite beams by increase of nanotube volume fraction. Moreover, formation of interphase with better mechanical properties than polymer matrix can improve buckling characteristics of nanocomposite beams. It was observed that temperature significantly affects the buckling load of nanocomposite beams.

## References

- [1] Dai, H. (2002). Carbon nanotubes: opportunities and challenges. *Surface Science*, 500(1-3), 218-241.
- [2] De Volder, M. F., Tawfick, S. H., Baughman, R. H., & Hart, A. J. (2013). Carbon nanotubes: present and future commercial applications. *science*, 339(6119), 535-539.
- [3] Popov, V. N. (2004). Carbon nanotubes: properties and application. *Materials Science and Engineering: R: Reports*, 43(3), 61-102.
- [4] Guo, P., Chen, X., Gao, X., Song, H., & Shen, H. (2007). Fabrication and mechanical properties of well-dispersed multiwalled carbon nanotubes/epoxy composites. *Composites science and Technology*, 67(15-16), 3331-3337.
- [5] Ahmadi, M., Ansari, R., & Rouhi, H. (2020). Studying buckling of composite rods made of hybrid carbon fiber/carbon nanotube-reinforced polyimide using multi-scale FEM. *Scientia Iranica*, 27(1), 252-261.
- [6] Zhu, B. K., Xie, S. H., Xu, Z. K., & Xu, Y. Y. (2006). Preparation and properties of the polyimide/multi-walled carbon nanotubes (MWNTs) nanocomposites. *Composites Science and Technology*, 66(3-4), 548-554.
- [7] So, H. H., Cho, J. W., & Sahoo, N. G. (2007). Effect of carbon nanotubes on mechanical and electrical properties of polyimide/carbon nanotubes nanocomposites. *European Polymer Journal*, 43(9), 3750-3756.
- [8] Qian, D., Dickey, E. C., Andrews, R., & Rantell, T. (2000). Load transfer and deformation mechanisms in carbon nanotube-polystyrene composites. *Applied physics letters*, 76(20), 2868-2870.
- [9] Jia, Y., Peng, K., Gong, X. L., & Zhang, Z. (2011). Creep and recovery of polypropylene/carbon nanotube composites. *International Journal of Plasticity*, 27(8), 1239-1251.
- [10] Rong, C., Ma, G., Zhang, S., Song, L., Chen, Z., Wang, G., & Ajayan, P. M. (2010). Effect of carbon nanotubes on the mechanical properties and crystallization behavior of poly (ether ether ketone). *Composites Science and Technology*, 70(2), 380-386.
- [11] Kundalwal, S. I., & Ray, M. C. (2014). Effect of carbon nanotube waviness on the effective thermoelastic properties of a novel continuous fuzzy fiber reinforced composite. *Composites Part B: Engineering*, 57, 199-209.
- [12] Mahmoudi, M. J., Maleki, M., & Hassanzadeh-Aghdam, M. K. (2018). Static bending and free vibration analysis of hybrid fuzzy-fiber reinforced nanocomposite Beam-A multiscale modeling. *International Journal of Applied Mechanics*, 10(05), 1850053.
- [13] Montazeri, A., Javadpour, J., Khavandi, A., Tcharkhtchi, A., & Mohajeri, A. (2010). Mechanical properties of multi-walled carbon nanotube/epoxy composites. *Materials & Design*, 31(9), 4202-4208.

- [14] Aragh, B. S., Barati, A. N., & Hedayati, H. (2012). Eshelby–Mori–Tanaka approach for vibrational behavior of continuously graded carbon nanotube-reinforced cylindrical panels. *Composites Part B: Engineering*, 43(4), 1943-1954.
- [15] Pakseresht, M., Ansari, R., & Hassanzadeh-Aghdam, M. K. (2020). Analyzing the effects of interphase on the effective damping properties of aligned carbon nanotube-reinforced epoxy nanocomposites using a micromechanical approach. *Proceedings of the Institution of Mechanical Engineers, Part L: Journal of Materials: Design and Applications*, 234(7), 910-923.
- [16] Hassanzadeh-Aghdam, M. K., Ansari, R., & Mahmoudi, M. J. (2019). Thermo-mechanical properties of shape memory polymer nanocomposites reinforced by carbon nanotubes. *Mechanics of Materials*, 129, 80-98.
- [17] Haghgoo, M., Ansari, R., & Hassanzadeh-Aghdam, M. K. (2018). Effective elastoplastic properties of carbon nanotube-reinforced aluminum nanocomposites considering the residual stresses. *Journal of Alloys and Compounds*, 752, 476-488.
- [18] Civalek, O., & Jalaei, M. H. (2020). Shear buckling analysis of functionally graded (FG) carbon nanotube reinforced skew plates with different boundary conditions. *Aerospace Science and Technology*, 99, 105753.
- [19] Mohamed, N., Mohamed, S. A., & Eltaher, M. A. (2020). Buckling and post-buckling behaviors of higher order carbon nanotubes using energy-equivalent model. *Engineering with Computers*, 1-14.
- [20] Wang, J. F., Cao, S. H., & Zhang, W. (2021). Thermal vibration and buckling analysis of functionally graded carbon nanotube reinforced composite quadrilateral plate. *European Journal of Mechanics-A/Solids*, 85, 104105.
- [21] Yas, M. H., & Samadi, N. (2012). Free vibrations and buckling analysis of carbon nanotube-reinforced composite Timoshenko beams on elastic foundation. *International Journal of Pressure Vessels and Piping*, 98, 119-128.
- [22] Rafiee, M., Yang, J., & Kitipornchai, S. (2013). Thermal bifurcation buckling of piezoelectric carbon nanotube reinforced composite beams. *Computers & Mathematics with Applications*, 66(7), 1147-1160.
- [23] Wattanasakulpong, N., & Ungbhakorn, V. (2013). Analytical solutions for bending, buckling and vibration responses of carbon nanotube-reinforced composite beams resting on elastic foundation. *Computational Materials Science*, 71, 201-208.
- [24] Shi, D. L., Feng, X. Q., Huang, Y. Y., Hwang, K. C., & Gao, H. (2004). The effect of nanotube waviness and agglomeration on the elastic property of carbon nanotube-reinforced composites. *J. Eng. Mater. Technol.*, 126(3), 250-257.
- [25] Tsai, J. L., Tzeng, S. H., & Chiu, Y. T. (2010). Characterizing elastic properties of carbon nanotubes/polyimide nanocomposites using multi-scale simulation. *Composites Part B: Engineering*, 41(1), 106-115.
- [26] Parashkevova, L., & Bontcheva, N. (2013). Micropolar-based modeling of size effects on stiffness and yield stress of nanoparticles-modified polymer composites. *Computational materials science*, 67, 303-315.
- [27] Yanase, K., Moriyama, S., & Ju, J. W. (2013). Effects of CNT waviness on the effective elastic responses of CNT-reinforced polymer composites. *Acta Mechanica*, 224(7), 1351-1364.
- [28] Shen, L., & Li, J. (2004). Transversely isotropic elastic properties of single-walled carbon nanotubes. *Physical Review B*, 69(4), 045414.
- [29] Yang, Q. S., He, X. Q., Liu, X., Leng, F. F., & Mai, Y. W. (2012). The effective properties and local aggregation effect of CNT/SMP composites. *Composites Part B: Engineering*, 43(1), 33-38.